SNR of swept SLEDs and swept lasers for OCT

Bart Johnson,* Walid Atia, Dale C. Flanders, Mark Kuznetsov, Brian D. Goldberg, Nate Kemp, and Peter Whitney

Axsun Technologies, Billerica, Massachusetts, USA

**bjohnson@axsun.com*

Abstract: A back-to-back comparison of a tunable narrow-band-filtered SLED (TSLED) and a swept laser are made for OCT applications. The two sources are similar in terms of sweep speed, tuning range and coherence length. A fundamental issue with a TSLED is that the RIN is proportional to 1/linewidth, meaning that the longer the coherence length, the higher the RIN and clock jitter. We show that the TSLED has an SNR limit that causes noise streaks at points of high reflection in images. The laser, which is shot noise limited, does not exhibit this effect. We add noise terms proportional to the sample power times reference power to standard swept source SNR expressions to account for the SNR limit.

OCIS codes: (110.4500) Optical coherence tomography; (110.4280) Noise in imaging systems; (140.6630) Superradiance, superfluorescence.

References and links

1. C. M. Eigenwillig, B. R. Biedermann, W. Wieser, and R. Huber, “Wavelength swept amplified spontaneous emission source,” Opt. Express **17**, 18794–18807 (2009).
2. “Noise sources in optical measurements,” W. V. Sorin, section A.4, 608-613 in *Fiber Optic Test and Measurement*, D. Derickson, ed. (Prentice Hall, 1998).
3. S. Shin, U. Sharma, H. Tu, W. Jung, and S. A. Boppart, “Characterization and analysis of relative intensity noise in broadband optical sources for optical coherence tomography,” IEEE Photon. Technol. Lett. **22(14)**, 1057–1059 (2010).
4. M. Kuznetsov, W. Atia, B. Johnson, and D. C. Flanders, “Compact ultrafast reflective Fabry-Perot tunable lasers for OCT imaging applications,” Proc. SPIE **7554**, 75541F1 (2010).
5. W. Drexler and J. G. Fujimoto, eds., “Swept light sources,” *Optical Coherence Tomography, Technology and Applications*, 2nd ed. (Springer, 2008) chap. 21, pp. 639–658.
6. B. Johnson, W. Atia, M. Kuznetsov, B. D. Goldberg, P. Whitney, and D. C. Flanders, “Analysis of a spinning polygon wavelength swept laser,” arXiv:1501.07003v2 (2015).
7. B.C. Johnson, W. Atia, M. Kuznetsov, and D. C. Flanders, “Passively mode locked swept lasers,” Photonics West 2013, Poster 8571-103, February 4, 2013, electronic copy available from authors.
8. B. C. Johnson, and D. C. Flanders, “Actively mode locked laser swept source for OCT medical imaging,” US Patent Application, US 20120162662 A1, (2012).
9. S. Slepneva, B. OShaughnessy, B. Kelleher, S.P. Hegarty, A. Vladimirov, H.-C. Lyu, K. Karnowski, M. Wojtkowski, and G. Huyet, “Dynamics of a short cavity swept source OCT laser,” Opt. Express **22** 18177–18185 (2014).
10. E. Avrutin and L. Zhang, “Dynamics of semiconductor lasers under fast intracavity frequency sweeping,” 14th Int. Conf. on Transparent Optical Networks (ICTON), 1-4 (2012).
11. S. H. Yun, G. J. Tearney, J. F. de Boer, N. Iftimia, and B. E. Bouma, “High-speed optical frequency-domain imaging,” Opt. Express **11**, 2953–2963 (2003).
12. M. A. Choma, M. V. Sarunic, C. Yang, and J. Izatt, “Sensitivity advantage of swept source and Fourier domain optical coherence tomography,” Opt. Express **11**, 2183–2189 (2003).
13. R. Leitgeb, C. K. Hitzenberger, and A. F. Fercher, “Performance of Fourier domain vs. time domain optical coherence tomography,” Opt. Express **11**, 889–894 (2003).

#260788 Received 8 Mar 2016; revised 2 May 2016; accepted 3 May 2016; published 13 May 2016

14. J. F. de Boer, B. Cense, B. H. Park, M. C. Pierce, G. J. Tearney, and B. E. Bouma, "Improved signal-to-noise ratio in spectral-domain compared with time-domain optical coherence tomography," Opt. Lett. **28**, 2067–2069 (2003).
15. M. Wojtkowski, "High-speed optical coherence tomography: basics and applications," Appl. Opt. **49(16)**, D30–D61 (2010).
16. *Fiber Optic Test and Measurement*, D. Derickson, ed. (Prentice Hall, 1998).
17. F. J. Harris, "On the use of windows for harmonic analysis with the discrete Fourier transform," Proc. IEEE, **66(1)**, 51–83 (1978).

1. Introduction

Swept tunable SLEDs (TSLED), where amplified spontaneous emission is filtered into a tunable narrow line, have a potential speed advantage over many swept lasers that depend on complex laser dynamics. Shot-noise limited performance has been demonstrated for a TSLED with 4 mm coherence length [1]. We show here results for a TSLED with a much longer coherence length (14 mm). One complicating factor for these devices is that the RIN is proportional to 1/Linewidth [1–3], meaning that the longer the coherence length, the noisier the device. The high noise also causes increased clock jitter. We show that high RIN and high clock jitter lead to noise components that increase with signal level, which means the TSLED device has an SNR limit.

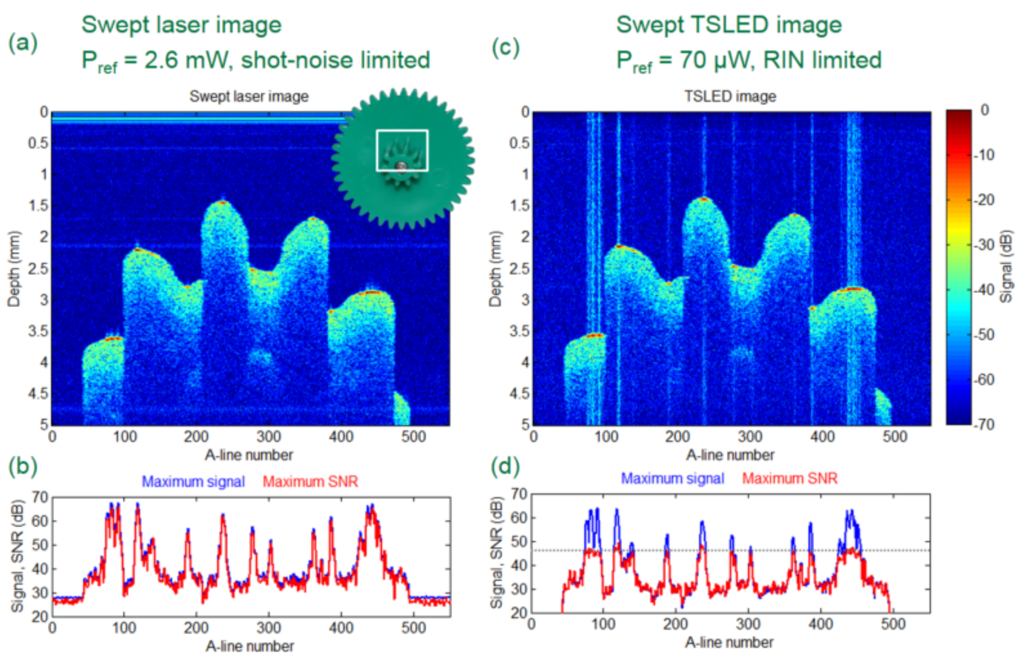

Fig. 1. Two OCT images of a plastic gear. (a) Image was taken with the swept laser at a high reference power so the shot-noise limit is reached. (b) Plot shows that the laser system SNR tracks the signal level. (c) Image was taken with the swept TSLED at the optimum reference power for RIN-limited operation. Vertical noise streaks occur because the system reaches its SNR limit for traces with very high peak signals. (d) Plot shows an SNR limit of approximately 46 dB for the TSLED, where the peak SNR ceases to track the peak signal power. The SNRs in plots (b) and (d) are the peak signal of each A-line minus the noise in a clear area of the A-line. The horizontal fixed pattern streak pixels in (a) were avoided in the noise calculation.

#260788 Received 8 Mar 2016; revised 2 May 2016; accepted 3 May 2016; published 13 May 2016

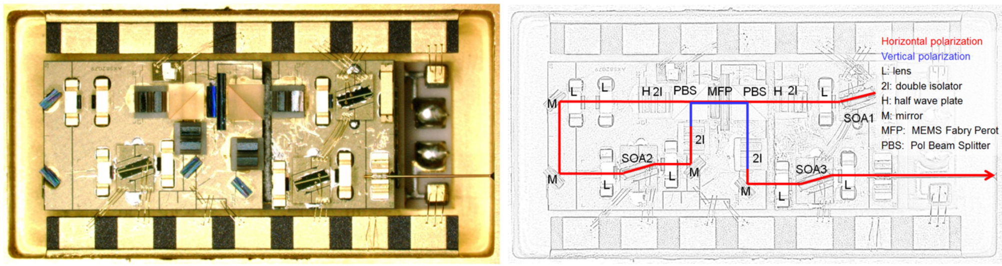

Fig. 2. Photograph and diagram showing the light path through the TSLED device.

We compare the performance of the swept TSLED with a swept laser [4, 5] that has similar performance in terms of tuning range, sweep speed, coherence, power output. The primary difference between the two sources is the mode of operation. The laser emits mode-locked pulses [5–10]; the TSLED emits narrow band optical noise.

Both the laser and TSLED can produce high quality images in terms of spatial resolution and dynamic range. The primary difference is that the TSLED image has vertical noise streaks that accompany high signal spots (Fig. 1, right). This is not a product of receiver saturation and signal clipping. It happens because an imaging system utilizing a TSLED has an SNR limit, in this case 46 dB (at 2.5mm depth). The main objective of this paper is to describe why the SNR limit occurs.

2. Comparison of TSLED and laser

Our TSLED contains a seed SOA (Semiconductor Optical Amplifier) and two amplification SOAs. The light passes through a 5-7 GHz wide MEMS tunable Fabry-Perot filter twice by polarization multiplexing (Fig. 2). The laser is constructed as described in [4]. The use of quantum well semiconductor optical amplifiers and other highly polarizing elements in the construction of both of these sources ensures that they both have a high degree of polarization.

We compare the TSLED with a standard Axsun swept laser with similar performance in sweep speeds, tuning ranges, coherence, and resolution (Table 1, Figs. 3-6). The main difference between these two swept sources is that the laser emits mode-locked pulses [5] and the TSLED is a narrow band noise source as is demonstrated in the spectrograms of the photodiode signal in Fig. 3.

Table 1. Comparison of laser and TSLED properties

Property	Swept Laser	Swept TSLED	Units
Emission	Mode-locked pulses	Filtered ASE	
Polarization	High DOP	High DOP	
Sweep rate	50	50	kHz
Retrace	blanked	blanked	
Average power	38	22	mW
Sampled bandwidth	16.8	16.8	THz
Sampling duty cycle	40	39	%
Wavelength band	1310	1310	nm
Tuning range	104	102	nm
Coherence	12	14	mm

#260788 Received 8 Mar 2016; revised 2 May 2016; accepted 3 May 2016; published 13 May 2016

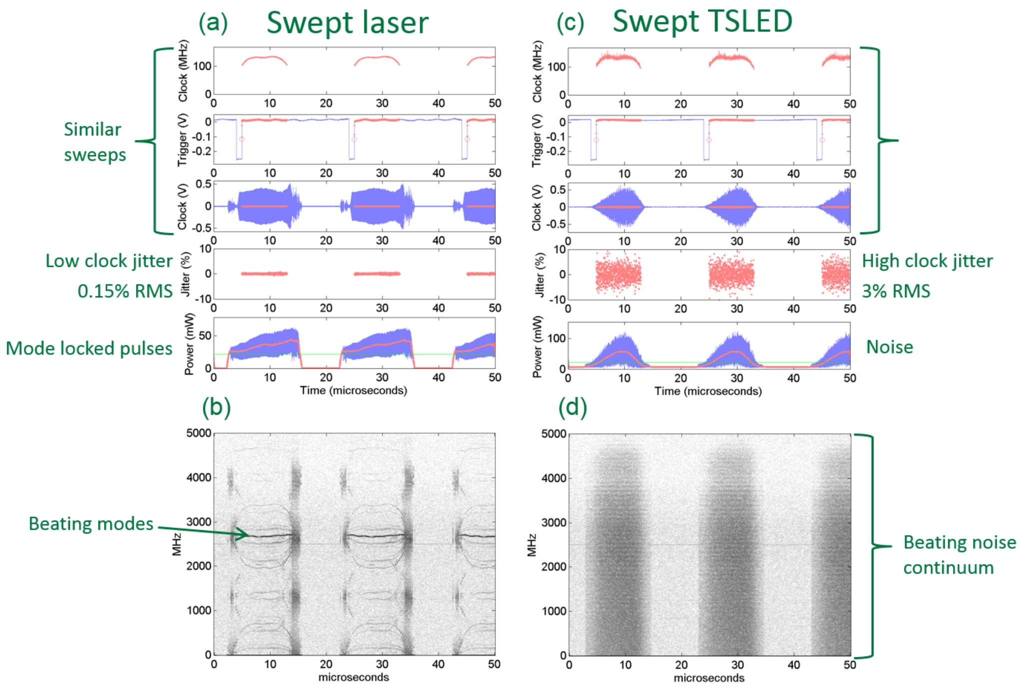

Fig. 3. Sweep data for the laser (a) and TSLED (c), including instantaneous clock frequency, sweep trigger, clock waveform, clock jitter (% of local period), and power output. The blue power trace has greater than 2.5 GHz bandwidth that shows mode-locked pulses for the laser, and wide-band noise for the TSLED. The red power traces show the power signal filtered to a 5 MHz bandwidth. The blue power traces are used to construct spectrograms for both devices which show beating modes at 2700 MHz for the laser (b) and broad band beat noise for the TSLED (d). The darker gray in the 0-70 MHz band of the TSLED spectrogram, compared to that of the laser, shows higher TSLED RIN within the OCT system balanced receiver bandwidth.

#260788 Received 8 Mar 2016; revised 2 May 2016; accepted 3 May 2016; published 13 May 2016

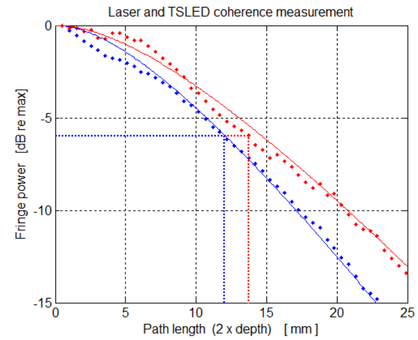

Fig. 4. Coherence measurements for the laser (12 mm) and the TSLED (14 mm). These measurements were made using a high-speed detector and greater than 2.5 GHz bandwidth oscilloscope. The signals themselves were used as both a ”clock” and as a ”signal” when determining the fringe amplitude. The measurements were fit with an 8.5 GHz Lorentzian^2 coherence function (see Table 2) for the laser (blue) and a 7.0 GHz Lorentzian^2 coherence fit for the TSLED (red).

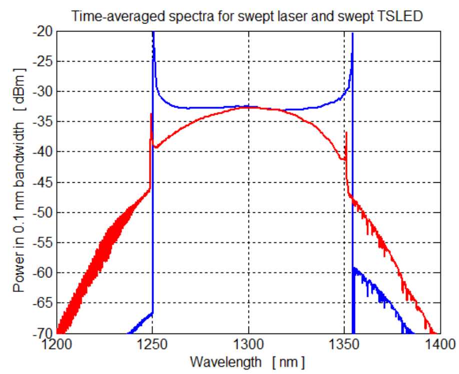

Fig. 5. Time averaged spectra for the swept laser and swept TSLED. The high ASE background in the case of the TSLED is due to the fact that SOA1 and SOA2 were blanked, but SOA3 was not, due to a limitation of the drive electronics. Both devices had similar tuning ranges.

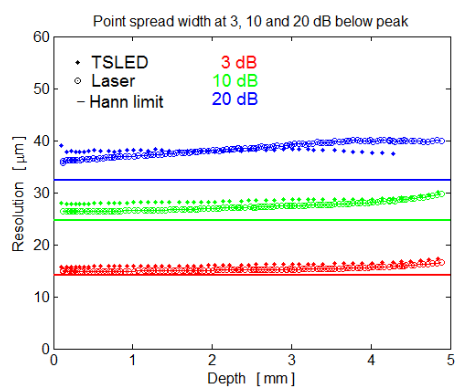

Fig. 6. Axial resolution measurements approach the transform limit for a Hann window for both the laser and the TSELD out to the Nyquist depth of 5 mm.

#260788 Received 8 Mar 2016; revised 2 May 2016; accepted 3 May 2016; published 13 May 2016

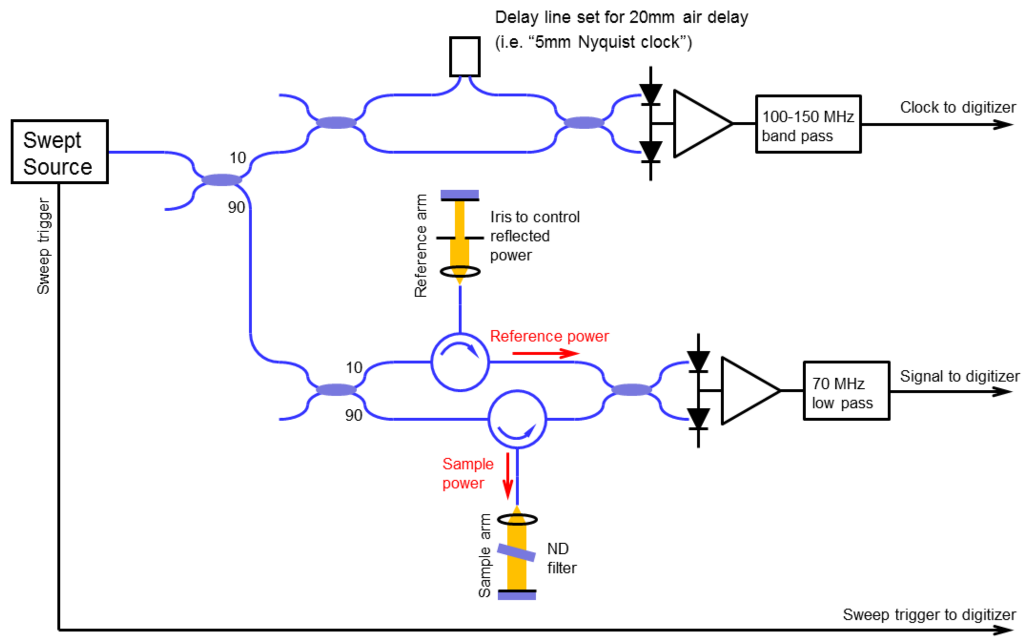

Fig. 7. System used for SNR and sensitivity measurements. For imaging, the sample arm was replaced by imaging optics with a galvo scanner. The diagram shows the sample and reference power definitions. The loss includes all optics downstream from the sample power point to the balanced receiver.

Table 2. Coherence Equations

Line Shape	Spectrum	Coherence function	RIN	Coherence Length
Lorentzian	$\frac{\frac{2}{\pi\Delta\nu}}{1+\left(\frac{2f}{\Delta\nu}\right)^2}$	$e^{-\pi\Delta\nu\|t\|}$	$\frac{2}{\pi\Delta\nu}$	$\frac{c\,ln(2)}{\pi\Delta\nu} = 0.221\frac{c}{\Delta\nu}$
(Lorentzian)^2	$\frac{\frac{4\sqrt{\sqrt{2}-1}}{\pi\Delta\nu}}{\left[1+\left(\sqrt{\sqrt{2}-1}\right)\left(\frac{2f}{\Delta\nu}\right)^2\right]^2}$	$\left(1+\frac{\pi\Delta\nu}{\sqrt{\sqrt{2}-1}}\|t\|\right)e^{-\frac{\pi\Delta\nu}{\sqrt{\sqrt{2}-1}}\|t\|}$	$\frac{4\sqrt{\sqrt{2}-1}}{\pi\Delta\nu}$	$0.344\frac{c}{\Delta\nu}$

3. SNR and sensitivity measurements

A conventional OCT interferometer (Fig. 7) is used in the imaging and signal-to-noise experiments. The digitizer is an Axsun design with a Camera Link digital interface and is based on the Texas Instruments ASD54RF63 12-bit 550 MS/s analog to digital converter. The balanced receiver for the signal channel is also an Axsun design. The technical specifications for the DAQ and receiver are more fully covered in [5]. The DAQ board directly samples on hardware clock pulses. No software resampling is involved. Signal and clock waves are aligned in time with added coaxial cabling in the clock arm to ensure full axial resolution at large depths.

For SNR and resolution measurements, A-lines are zero padded to 10x the 1024 sample length (10240) to prevent scalloping loss and allow accurate point-spread width measurements. In addition, the Fourier transformed power signals for 100 A-lines are averaged and then converted to dB. Since the phase information is removed before averaging, the resulting noise floor becomes a better estimate for the single-sweep noise floor.

#260788 Received 8 Mar 2016; revised 2 May 2016; accepted 3 May 2016; published 13 May 2016

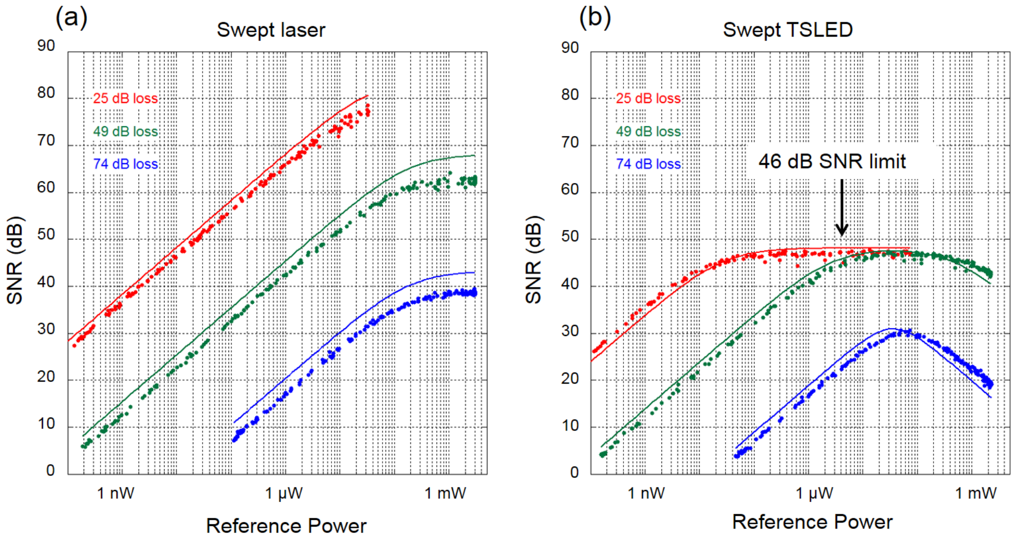

Fig. 8. SNR data at a depth of 2.5 mm for the swept laser (a) and the swept TSLED (b). The SNR rise and leveling off with reference power for the laser shows that the shot-noise limit is reached. The laser can achieve an SNR of almost 80 dB before the onset of receiver saturation and clipping. The peak in the blue TSLED SNR curve at 70 μW indicates RIN-limited behavior. In addition, at higher sample powers (lower loss), a 46 dB SNR limit is observed. Experimental SNR data (dots) are compared with theoretical curves (solid lines) from Eq. (5) using the parameters in Table 3.

Table 3. Noise model parameters for swept laser and swept TSLED

Property	Symbol	Swept Laser	Swept TSLED	Units
Detector quantum efficiency	η	0.9	0.9	
Hann window processing loss	η_{Proc}	0.67	0.67	
Noise equivalent power	NEP	8	8	$pW/\sqrt{Hz}$
Relative intensity noise	RIN	<-150	-106	dB/Hz
Common mode rejection	$CMRR$	-30	-30	dB
Phase noise at 2.5 mm depth	$RIN_{\Delta\phi}$	<-135	-103	dB/Hz
Receiver bandwidth	B	70	70	MHz
Number of samples	N	1024	1024	

Sensitivity is the smallest reflection that can be seen by an OCT system, expressed in negative dB. By definition, the SNR is one when presented with that small reflection. In practice, the SNR needs to be measured with high optical loss in the optical system to simulate a low reflectivity. Thus the sensitivity is the SNR plus the optical loss used in the measurement.

The SNR and sensitivity data (Figs. 8, 9) shows very different behavior for the shot-noise limited laser and the RIN-limited and SNR-limited TSLED. Laser data higher than 80 dB was not obtained because of receiver saturation. Experimental SNR data were compared with Eq. (5) using the parameters in Table 3. In the case of the TSLED, these fits show support for the new signal-dependent noise terms. These new noise terms are proportional to the P_rP_s product, where P_r and P_s are the optical reference and sample powers.

Plotting SNR+Loss allows the sensitivity to be measured (Fig. 9). The sensitivity is correctly determined at high loss for the TSLED since by definition it is the response to low light levels.

#260788 Received 8 Mar 2016; revised 2 May 2016; accepted 3 May 2016; published 13 May 2016

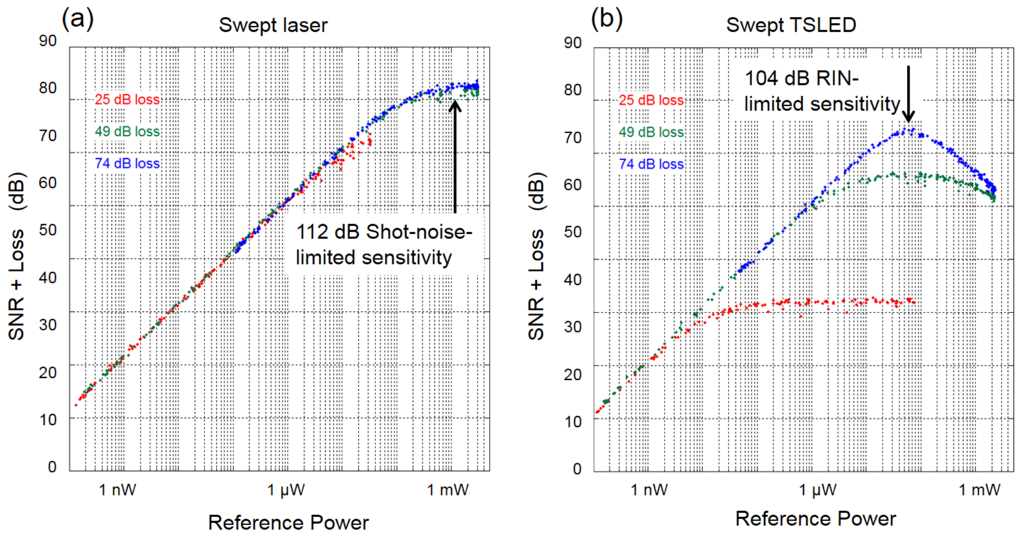

Fig. 9. Sensitivity data at a depth of 2.5 mm for the swept laser (a) and the swept TSLED (b). The laser has a shot-noise-limited 112 dB sensitivity with 11.5 mW sample power. The TSLED is RIN limited with a 104 dB sensitivity for 6.8 mW sample power. Note that the TSLED sensitivity must be measured with high loss to prevent the SNR limit from affecting the results.

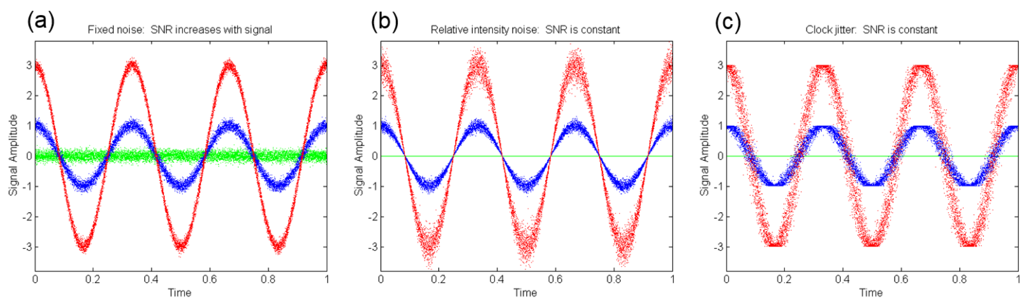

Fig. 10. Simulated interference waveforms illustrating signal-to-noise processes. (a) Fixed noise. SNR goes up with signal amplitude. (b) Effect of interference RIN where SNR does not vary with signal amplitude. (c) Effect of clock jitter where SNR does not vary with signal amplitude.

The laser, having and very large SNR limit, is not sensitive to the loss level.

With the exception of [11], most Fourier domain SNR [12–15] calculations do not include signal-power-dependent noise (proportional to P_rP_s). We have added two noise terms below to account for interference RIN and clock jitter. A balanced receiver can remove RIN from a reference beam by itself, but adding an interfering sample beam unbalances it. This effect, usually negligible, is important for the TSLED. The clock jitter noise term is depth dependent, as discussed in Section 5.

4. Physical picture of the noise sources

Most OCT noise models assume the noise is independent of signal amplitude, as in Fig. 10(a). There are two ways noise can become proportional to signal amplitude. Figure 10(b) shows the

#260788 Received 8 Mar 2016; revised 2 May 2016; accepted 3 May 2016; published 13 May 2016

output of a balanced receiver with high RIN. A balanced receiver is thought of as a device that cancels RIN, which is true when $P_r \gg P_s$. In that case the detectors are nearly balanced and the RIN on the reference beam is canceled. At higher sample powers, the detectors become unbalanced during constructive and destructive interference. In that case, RIN is not canceled and the signal and noise increase together yielding a constant SNR. We call this the "interference RIN" to differentiate it from the usual RIN seen on a simple photodetector with no interferometer. The interference RIN of the TSLED is compared with that of the laser in Fig. 11.

Figure 10(c) shows the effect of clock jitter. Jitter in the clock means that sampling of the signal doesn't happen at the exact intended k values, but that there is a random component to the timing. When sampling on the up-slope or down-slope of a sinusoidal signal, the clock jitter translates into amplitude noise through a phase-to-AM conversion process.

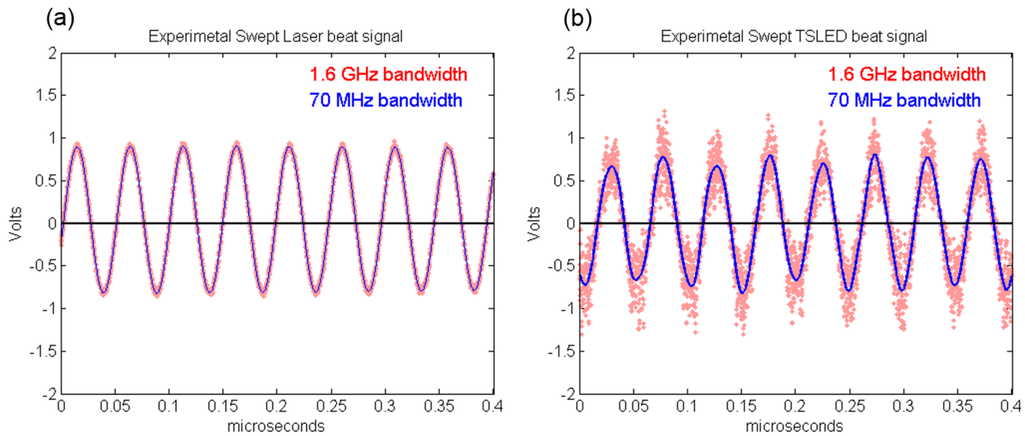

Fig. 11. Beat signals on a 1.6 GHz bandwidth balanced receiver for the swept laser (a) and swept TSLED (b). The signals are then numerically filtered to 70 MHz to show how they appear in the OCT system experiments. The TSLED signal shows high RIN at the beat peaks that is not eliminated by the balanced receiver.

5. Clock jitter model

We simulate the effect of clock jitter by assuming a signal of $s(k) = (4/N)cos[\pi(z/z_{max})k]$. The depth is z and the Nyquist fold-over depth is z_{max}. $k = 0, 1, , N-1$. When simulating clock jitter, k is replaced by $k + \delta k(k)$ where δk is a Gaussian random variable. For example, for 10% RMS clock jitter, the standard deviation of δk is $\sigma_{\delta k} = 0.1$. In Fig. 12, the power spectrum, using a Hann window $[H(k) = 0.5 - 0.5\ cos(2\pi k/N)]$, of the above function is computed 100 times, averaged, and converted to dB.

The things to note about Fig. 12 are that the resolution is not affected by Gaussian clock jitter (experimentally confirmed in Fig. 6) and that the noise floor increases with sample depth. This behavior is summarized in Fig. 13 where the signal and noise are plotted versus depth for three different clock jitter amplitudes. The dots represent data points from the type of simulation shown in Fig. 12, and the solid lines represent the closed form expressions Eqs. (3,4).

The amplitude noise signal due to clock jitter is:

$$n(k) = s(k + \delta k(k)) - s(k) \approx -\frac{4}{N}\left[\pi \frac{z}{z_{max}} \delta k\right] \sin\left[\pi \frac{z}{z_{max}} k\right] \tag{1}$$

The energy in the noise signal assuming a Hann window is:

#260788 Received 8 Mar 2016; revised 2 May 2016; accepted 3 May 2016; published 13 May 2016

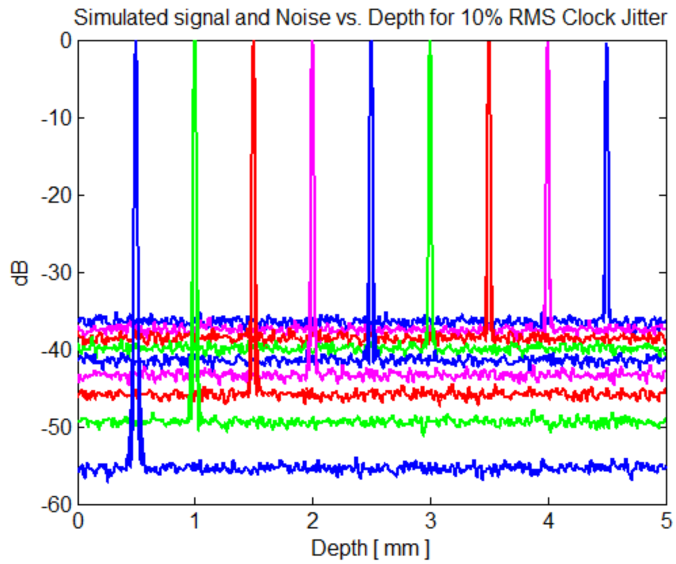

Fig. 12. Simulated signal and noise from clock jitter model (10% RMS jitter). One hundred power spectra with random clocks were averaged and then converted to dB to create each trace.

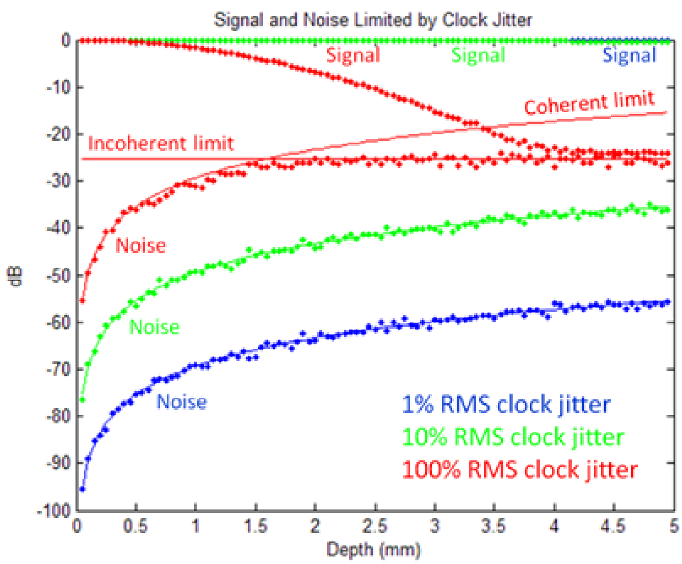

Fig. 13. This plot summarizes the data in Fig. 12 for three different levels of clock jitter. The dots are from the simulation shown in Fig. 12 and the solid curves are from Eq. (3). The incoherent limit line is from Eq. (4). The noise floor increases 20 dB for every factor of 10 in clock jitter until the incoherent limit is reached.

#260788 Received 8 Mar 2016; revised 2 May 2016; accepted 3 May 2016; published 13 May 2016

$$\sum_k n^2(k) H^2(k) = \frac{3}{N}\left(\pi \frac{z}{z_{max}}\right)^2 \sigma_{\delta k}^2 \tag{2}$$

The noise signal in each bin of the FFT can be calculated using Parsevals theorem and the fact that the noise is white. The noise in the ”coherent limit”, where the clock jitter is much less than one period of the signal, is

$$\text{Noise for coherent limit} = 10\log_{10}\left[\frac{3}{N}\left(\pi \frac{z}{z_{max}}\right)^2 \sigma_{\delta k}^2\right] \text{ dB} \tag{3}$$

The “incoherent limit” is where the jitter is much more than one signal period. It can be computed following a procedure similar to one the above.

$$\text{Noise for incoherent limit} = 10\log_{10}\left[\frac{3}{N}\right] \text{ dB} \tag{4}$$

These expressions are plotted in Fig. 13 along with data points from the numerical simulation.

6. Expression for SNR

An expression for the signal-to-noise ratio is shown in Eq. (5). Much of the notation is borrowed from [11], but a term in the denominator accounting for the phase noise [16] is added. The phase noise coefficient $RIN_{\Delta\phi}(z)$ is depth dependent. The five noise terms in the denominator of Eq. (5) are (1) the photoreceiver fixed noise, (2) shot noise, (3) RIN, (4) interference RIN, (5) clock jitter noise.

$$SNR = \frac{N\eta_{Proc} P_r P_s}{\left[NEP^2 + 2\frac{h\nu}{\eta}\left(P_r + P_s\right) + RIN \cdot CMRR\left(P_r^2 + P_s^2\right) + 2\ RIN \cdot P_r P_s + 2\ RIN_{\Delta\phi}\left(z\right) P_r P_s\right] B} \tag{5}$$

P_r = reference beam power
P_s = sample beam power
η = detector quantum efficiency
η_{Proc} = digital processing loss [17]
$h\nu$ = photon energy
NEP = noise equivalent power of the receiver
RIN = relative intensity noise coefficient
$CMRR$ = common mode rejection ratio of the balanced receiver
$RIN_{\Delta\phi}(z)$ = depth-dependent phase noise coefficient
B = bandwidth of optical receiver (1/2 sampling rate)
N = number of samples

In cases where the $P_r P_s$ product is high, the SNR reaches the following limit:

$$\text{SNR limit} = \frac{N\eta_{Proc}}{2\ \left[RIN + RIN_{\Delta\phi}\left(z\right)\right] B} \tag{6}$$

The shot-noise limit for the swept laser is:

$$\text{Shot-noise limited sensitivity} = \frac{N\eta_{Proc} P_s}{\left[2\frac{h\nu}{\eta}\right] B} \tag{7}$$

#260788 Received 8 Mar 2016; revised 2 May 2016; accepted 3 May 2016; published 13 May 2016

The RIN-limited sensitivity for the TSLED occurs when $NEP^2 = RIN \cdot CMRR \cdot P_r^2$. At this point the relative intensity noise equals the fixed receiver noise and the SNR and sensitivity reach a peak as seen in the blue curve of Fig. 8(b). In this low sample power and high RIN regime, the detector noise and RIN dominate the noise sources.

$$\text{RIN limited sensitivity} = \frac{N\eta_{Proc} P_r P_s}{2\, NEP^2\, B} \tag{8}$$

An SNR limit may be due to high interference RIN or high phase noise (i.e. clock jitter). In an imaging system, the reference power will be fixed and the SNR limit may be reached at points of high reflection (P_s becomes high) and a noise streak will occur because of the increase in the noise floor across all depths. Note that the interference RIN and phase noise powers are proportional to the $P_r P_s$ product. Both sample and reference beams need to be present for these types of noise to occur. Blocking the sample or reference beams while monitoring the noise floor is an important diagnostic for these types of noise.

7. Experimental comparison with the model

The measured TSLED RIN parameters of Table 3 were found through parameterized fits of Eq. (5) to the data in Fig. 8. Limits on the laser RIN parameters were found through similar fits.

Various calculated and measured noise parameters are compared in Table 4. The parameters match reasonably well. With a TSLED Lorentzian linewidth of $\Delta\nu$ = 7 GHz, the expected RIN (see Eq. (9) and Table 2) is -99 dB/Hz. The measured number from SNR curve fitting is -106 dB/Hz. Saturated amplification in a SOA, as is the case in our TSLED, can reduce the RIN, although the bandwidth scaling remains in effect [3]. The intact bandwidth scaling means that there will still be a tradeoff between coherence length and noise performance for a

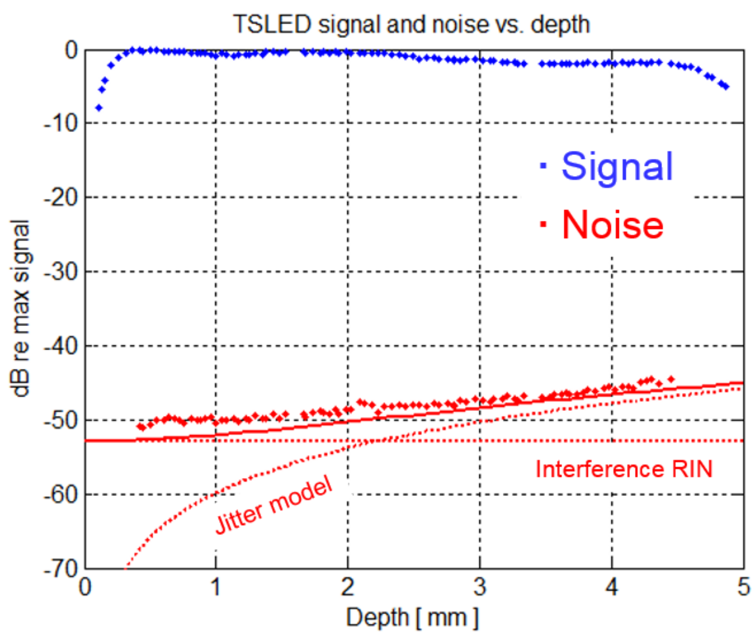

Fig. 14. Swept TSLED signal and noise as a function of depth when run well into the SNR-limited region. Note that the noise floor rises with depth, supporting the clock jitter analysis.

#260788 Received 8 Mar 2016; revised 2 May 2016; accepted 3 May 2016; published 13 May 2016

TSLED [1–3].

$$\text{Spontaneous emission source RIN} = \frac{4\sqrt{\sqrt{2}-1}}{\pi \Delta \nu} \tag{9}$$

The clock jitter model predicts an SNR limit that decreases with depth, as shown in Fig. 14. The predicted curves are derived from Eqs. (6 and 3) with a clock jitter of $\sigma_{\delta k} = 0.03$ (see Fig. 3). It should be noted that signals have jitter too, but it is much less than that of the clock since the clock interferometer has a much longer path mismatch. Therefore the jitter effect is dominated by the clock, as described in Section 5.

Table 4. Noise model parameters for swept laser and swept TSLED

Measurement (fit to Figs. 3, 8, 14)	Value	Calculation	Value
Laser sensitivity	112 dB	Shot noise limit Eq. (7)	115 dB
TSLED sensitivity at 2.5 mm	104 dB	RIN-limited Eq. (8)	107 dB
TSLED RIN	-106 dB/Hz	Eq. (9)	-99 dB/Hz
TSLED $RIN_{\Delta\phi}(2.5mm)$	-103 dB/Hz	Eq. (3), Fig. 3	-101 dB/Hz
TSLED SNR limit at 2.5 mm	46 dB	Eq. (6)	48 dB/Hz

8. Conclusion

We have added new noise sources to the expression for SNR that scale in proportion to $P_r P_s$ which account for interference RIN and clock jitter noise. These sources scale differently than standard RIN (proportional to P_r^2 and P_s^2), and shot noise (proportional to P_r and P_s).

A measurement of the SNR limit, as well as the sensitivity, would be included in a full characterization of an OCT system. A low SNR limit does not necessarily mean the sensitivity of an OCT system is poor. The TSLED described here has a respectable sensitivity, only 6 dB less than the shot noise limit, but a very low SNR limit. The practical reason for wanting a high SNR limit is to prevent streaks in the image where points of high reflection are accompanied by high background noise, obscuring subtle features in the A-line.

The clock jitter problem could be mitigated by software resampling, which would remove the "jitter model" noise component in Fig. 14. However, the "interference RIN" component would remain and the SNR limit for the TSLED would still be low.

The swept laser and swept TSLED devices are bookends for a continuum of source behavior. For example, spinning polygon lasers, which pulse chaotically [6], fall between these two cases in noise behavior. They exhibit an SNR limit, but not as severe as that of the TSLED.

There is a trade-off between coherence length and RIN for the TSLED. This was also pointed out in [1], but our device, with its longer coherence length, is a more extreme example.

Interference RIN and clock jitter lead to an SNR limit that can cause noise streaking in OCT images. We have augmented the mathematical expression for SNR in swept sources with noise terms including these two effects that accounts for the SNR limit.

#260788 Received 8 Mar 2016; revised 2 May 2016; accepted 3 May 2016; published 13 May 2016